Available online at www.sciencedirect.com
ScienceDirect
Current Applied Physics 9 (2009) 274–277
Current Applied Physics
An official journal of the KPS
www.elsevier.com/locate/cap
www.kps.or.kr

Capacitive discharge mode transition in moderate and atmospheric pressure

Se Youn Moon, J.K. Rhee, D.B. Kim, B.M. Gweon, W. Choe *

Department of Physics, Korea Advanced Institute of Science and Technology, 335 Gwahangno, Yuseong-gu, Daejeon 305-701, Republic of Korea

Received 18 February 2008; accepted 21 February 2008
Available online 29 February 2008

Abstract

Current–voltage characteristics of α- and γ-modes were investigated in moderate and atmospheric pressure capacitive discharges. The α- and γ-modes, the co-existence of both modes, and the α- to γ- and γ- to α-mode transitions were observed with the changes in voltage, current, and plasma volume. Changing of gas pressure, (100–760) Torr, the α to γ and the γ to α transition occurred with respect to input power increasing and decreasing, respectively. The hysteresis in current and voltage curve was observed and became more evident at higher pressure. Using a simple electrical circuit model, the relation between the gas pressure and the α-sheath thickness before mode transition was described.

PACS: 52.50.Qt; 52.77.Fv; 52.80.Pi

Keywords: Atmospheric pressure plasma; Discharge mode; Mode transition

1. Introduction

Attentions to atmospheric pressure glow discharge (APGD) plasmas have increased due to their numerous advantages, such as exclusion of expensive high vacuum equipments, simple operation, and various application targets [1–3]. One of the widely employed APGD sources is the radio-frequency (RF) capacitively-coupled discharge source, because of its relatively low breakdown voltage at the atmospheric pressure and the extensive employment in industries such as micro-circuit manufacturing and material treatments [3–5]. For such RF capacitive discharges, two different discharge modes of α and γ and the mode transition between the two have been studied for gas pressures from 10 mTorr to several tens of Torr [5–8]. Recent investigations also reported the existence of the γ-mode and the α–γ mode transition at the atmospheric pressure [9–11]. However, not much work has been pursued in the moderate to atmospheric pressure range. It is considered that studies on discharge modes is a prerequisite not only in understanding the plasma properties but also in industrial application of the plasmas because the plasma characteristics appear very differently in this pressure range. In this work, therefore, the properties of the α- and γ-mode and the forward and the reverse transitions between the two modes were studied in the gas pressure ranging from 100 Torr to 760 Torr. In addition, the pressure effects on the α-sheath thickness, which was obtained by a simple circuit model, was investigated.

2. Experimental setup

Fig. 1a illustrates a schematic of the experimental setup under study. The discharge source has two parallel copper electrodes with the same diameters of 60 mm which was cooled by chilled water. The bottom electrode was powered by a 13.56 MHz RF supply (Dressler Cesar 1312) through an impedance matching network. The power range was between 10 and 300 W. A current probe (Tektronix

* Corresponding author.
E-mail address: wchoe@kaist.ac.kr (W. Choe).

1567-1739/$ - see front matter
doi:10.1016/j.cap.2008.02.008

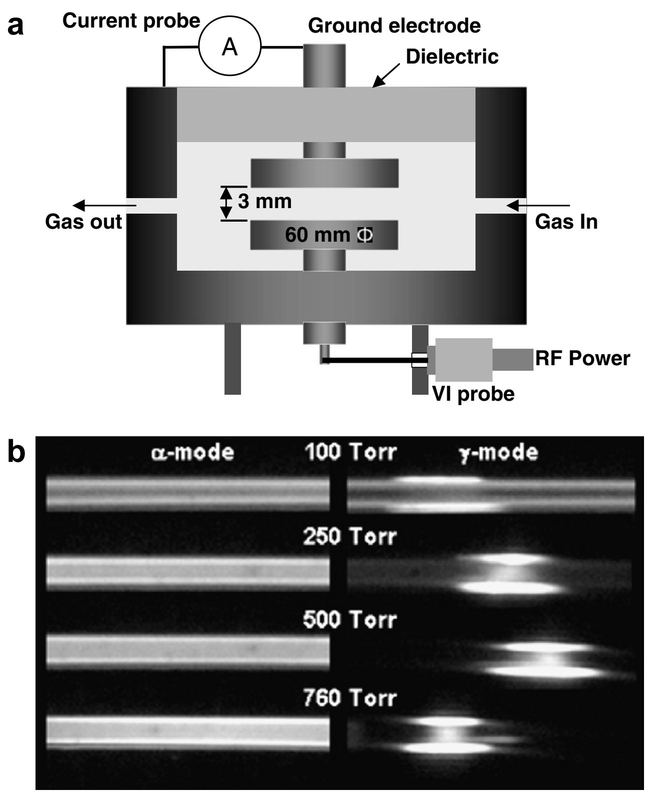

Fig. 1. (a) A Schematic of the experimental setup, and (b) discharge images of the α- and the γ-modes at 100, 250, 500, and 760 Torr, respectively.

TCP202), a voltage probe (Tektronix P6015A), and an impedance analyzer (MKS VI-probe 4100) with a digital oscilloscope (Tektronix TDS3012) were used for electrical measurements. A 99.99% purity helium gas was introduced into the chamber, of which pressure was controlled by pressure instruments (Pfeiffer Vacuum, Piezo gauge APR260, single gauge reader TPG261). During experiments, the pressure was sustained without additional gas feeding or pumping, and the discharge gap was fixed at 3 mm.

As indicated in Fig. 1b, α-mode and γ-mode were observed. As similarly observed in other experiments, the α-mode showed a relatively brighter region closer to the electrode, and a dark region between the bright region and the electrode. For the γ-mode, on the other hand, the brightest region existed at the electrode due to intensive negative glow, and the plasma volume was contracted [5,7]. The difference between the two discharge modes was resulted from the discharge sustaining mechanism. The ionization of the α-mode is mainly attributed to the bulk plasma electrons, but the ionization of the γ-mode is maintained by the secondary electrons emitted from the electrode [5,12]. At high gas pressure, the sheath breakdown is known to be responsible for α–γ mode transition [6,9].

3. Results and discussions

As shown in Fig. 2a where the normalized visible emission intensity obtained from the image-processed photograph taken at 250 Torr, both discharge modes were simultaneously seen inside the discharge gap, and the intensity profile of each mode corresponded to that of each singly existing mode. Up to about 500 Torr, the γ-mode coexisted with the α-mode, and the γ-mode discharge area was slightly expanded with increasing gas pressure and/or input power. The co-existence of both discharge modes can be explained by the inversion of the normal voltage of each mode [5]. When breakdown occurs, a normal glow α-discharge is sustained with a normal voltage $V_{\alpha,n}$ until the excitation of an abnormal glow discharge [9]. As the discharge experiences α- to γ-mode transition ($\alpha \rightarrow \gamma$) at higher voltage, the discharge area shrinks. However, the normal voltage $V_{\gamma,n}$ is applied throughout the whole area between the electrodes. If $V_{\alpha,n} > V_{\gamma,n}$, only a localized γ-mode appears. On the other hand, if $V_{\alpha,n} < V_{\gamma,n}$, $V_{\gamma,n}$ is sufficiently high to maintain both the α-discharge and the γ-discharge [5]. As shown in Fig. 2b where $V_{\alpha,n}$ and $V_{\gamma,n}$ are plotted with respect to pressure, $V_{\alpha,n} < V_{\gamma,n}$ below about 500 Torr in this experiment, resulting in the co-existence of both modes as demonstrated in Fig. 1b. Three

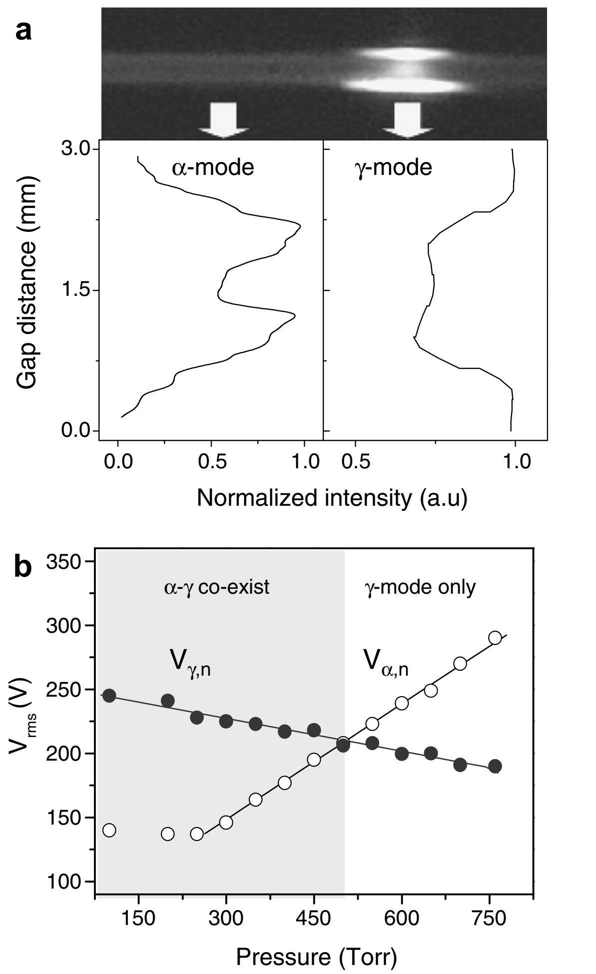

Fig. 2. (a) The normalized visible emission intensity profile of the α-mode (left) and the γ-mode (right) at 250 Torr when both modes co-exist. (b) Gas pressure effects on the normal glow discharge voltages of the α-mode (–○–, $V_{\alpha,n}$) and the γ-mode (–●–, $V_{\gamma,n}$).

points of $V_{\alpha,n}$ less than 300 Torr in Fig. 2b represent the voltages at the minimum input power where the discharge just became an abnormal glow.

Fig. 3 depicts a typical current (I) versus voltage (V) characteristic curve at various pressure, (a) 100 Torr, (b) 250 Torr, (c) 500 Torr, and (d) 760 Torr. As the current was increased with increasing input power $P_{\rm in}$, the discharge voltage and current were also increased. At a certain current $I_{\alpha\gamma}$ and voltage $V_{\alpha\gamma}$ (0.63 A and 272 V at 100 Torr), the $\alpha \rightarrow \gamma$ mode transition occurred, which was accompanied by a drop of discharge voltage, a reduction of the I–V phase angle, and a contraction of the discharge volume. After the γ-mode onset, raising $P_{\rm in}$ brought about a continuous increase of the current. In addition, decrease of $P_{\rm in}$ resulted in a significant current drop with a little change in the discharge voltage or a normal glow voltage $V_{\gamma,n}$. With a further $P_{\rm in}$ decrease, the discharge was changed from the γ- to the α-mode (with $I_{\gamma\alpha}$ of 0.61 A and $V_{\gamma\alpha}$ of 290 V at 100 Torr). As shown in Fig. 3, the more distinct hysteresis in current and voltage was observed at the higher pressure.

The pressure effects on the mode transition voltage and current are shown in Fig. 4. Here $V_{\alpha\gamma}$, $I_{\alpha\gamma}$, $V_{\gamma\alpha}$, and $I_{\gamma\alpha}$ are defined by the voltage and current at the $\alpha \rightarrow \gamma$ and the $\gamma \rightarrow \alpha$ mode transition, respectively. The $\alpha \rightarrow \gamma$ transition voltage $V_{\alpha\gamma}$ was increased with the gas pressure, similarly to the Paschen curve for the gas breakdown. In the $\gamma \rightarrow \alpha$ transition case, however, the transition voltage $V_{\gamma\alpha}$ decreased as the gas pressure was increased. It is because at the higher pressure, abundant electrons produced during the γ-discharge transfer more energy to neutrals by electron–neutral collisions, requiring a lower α-discharge excitation voltage. In case of discharge current versus pressure seen in Fig. 4b, $I_{\gamma\alpha}$ is lower than $I_{\alpha\gamma}$ because the electron density of the γ-mode is larger than that of the α-mode [12]. Especially, $I_{\gamma\alpha}$ was larger under 500 Torr range, which was due to the discharge current addition resulted from the co-existence of the α- and the γ- modes.

Finally, the α-sheath thickness d_α just before the $\alpha \rightarrow \gamma$ mode transition was evaluated for further understanding of the pressure effects on the discharge mode transition. A simple series-circuit model, composed of a resistor for bulk plasma and a parallel plate capacitor for sheath, was used as suggested in Refs. [8–10]. Hence, d_α is an averaged capacitive sheath width which was evaluated from the reactance ($X = 1/\omega C$, $d_\alpha = \epsilon_0 A/2C$ where $\omega = 2\pi\times$ 13.56 MHz, A is discharge area, and ϵ_0 is permittivity of free space) using the measured I, V, and phase angle

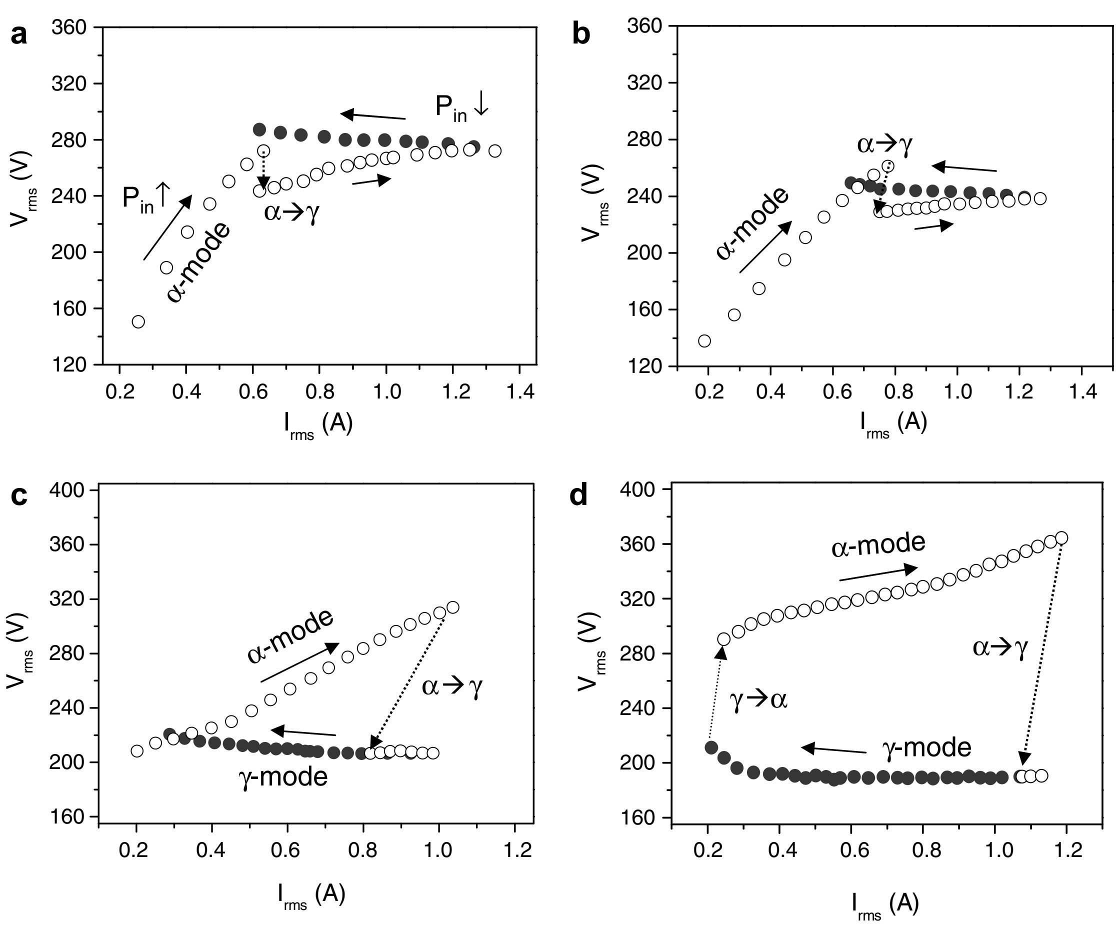

Fig. 3. I–V curves for (a) 100 Torr, (b) 250 Torr, (c) 500 Torr, and (d) 760 Torr were obtained as increasing (○) and decreasing (●) input power levels denoted as $P_{\rm in}$.

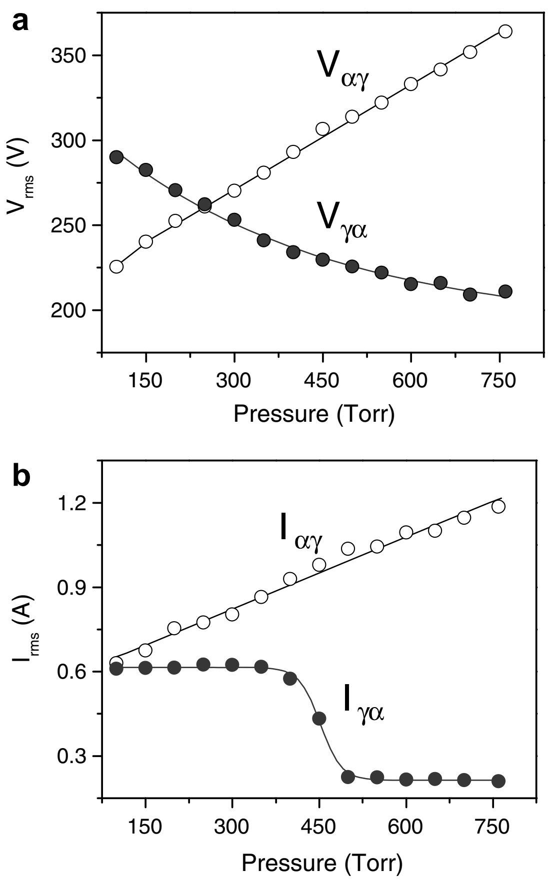

Fig. 4. (a) The transition voltage and (b) current at different gas pressure. Subscripts $\alpha\gamma$ and $\gamma\alpha$ denote the α to γ and γ to α mode transition, respectively.

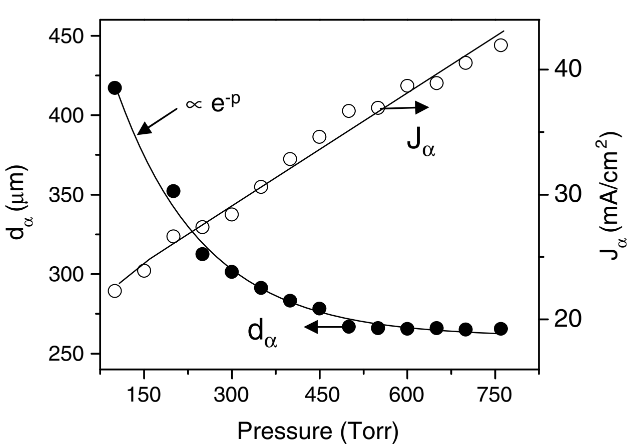

Fig. 5. Dependence of α-sheath thickness d_α (–•–) and current density J_α (–○–) on the gas pressure. d_α was evaluated from the measured current, voltage, and phase angle using a simple R–C circuit model. As the gas pressure, p, was raised, linear increase of J_α ($J_\alpha \propto p$) resulted in an exponential decrease of d_α ($d_\alpha \propto e^{-p}$).

between them [8]. As depicted in Fig. 5, $d_\alpha \propto \exp(-p)$ where p is the gas pressure. The α-sheath thickness d_α was decreased because of the increased discharge current density J_α of the α-mode [9,13].

4. Summary

In summary, the characteristics of discharge modes, the α and γ, were investigated for the 13.56 MHz RF capacitively-coupled helium plasma in the moderate and atmospheric pressure range. The mode transition of $\alpha \to \gamma$ and $\gamma \to \alpha$ at a specific voltage and current was accompanied by a change in voltage, current, phase angle, and plasma volume. In all pressure ranges, the hysteresis between the forward and the reverse mode transitions were observed, and it became more significant as the pressure was increased. The co-existence of the α and γ-modes was observed under about 500 Torr, which was resulted from the lower $V_{\alpha,n}$ than $V_{\gamma,n}$. The transition voltage and current at various gas pressure was also investigated for the $\alpha \to \gamma$ and $\gamma \to \alpha$ mode transitions. $V_{\alpha\gamma}$ was increased as the gas pressure was raised, which shows a similar trend as in the right hand side of the Paschen curve. A simple resistor–capacitor circuit model demonstrated that the sheath thickness just before the $\alpha \to \gamma$ mode transition was proportional to $\exp(-p)$.

Acknowledgements

This work was supported by Defense Acquisition Program Administration and Agency for Defense Development under the contract UD060005AD.

References

[1] J. Park, I. Henins, H.W. Herrmann, G.S. Selwyn, J. Appl. Phys. 89 (2001) 20.
[2] S.Y. Moon, B.K. Kang, W. Choe, Appl. Phys. Lett. 84 (2004) 188.
[3] G.S. Selwyn, H.W. Herrmann, J. Park, I. Henins, Contrib. Plasma Phys. 6 (2001) 610.
[4] S.Y. Moon, J.W. Han, W. Choe, Thin Solid Films 506–507 (2006) 355.
[5] Y.P. Raizer, M.N. Shneider, N.A. Yatsenko, Radio-Frequency Capacitive Discharges, CRC Press, Boca Raton, London, New York, Washington DC, 1995.
[6] V. Lisovskiy, J.P. Booth, K. Landry, D. Douai, V. Cassagne, V. Yegorenkov, Phys. Plasma. 13 (2006) 103505.
[7] P. Vidaud, S.M.A. Durrani, D.R. Hall, J. Phys. D: Appl. Phys. 21 (1988) 57.
[8] V.A. Godyak, R.B. Piejak, B.M. Alexandrovich, IEEE Trans. Plasma Sci. 19 (1991) 660.
[9] S.Y. Moon, J.K. Rhee, D.B. Kim, W. Choe, Phys. Plasmas 13 (2006) 033502-1.
[10] J.J. Shi, X.T. Deng, R. Hall, J.D. Punnett, M.G. Kong, J. Appl. Phys. 94 (2003) 6303.
[11] H.B. Wang, W.T. Sun, H.P. Li, C.Y. Bao, X.Z. Zhang, Appl. Phys. Lett. 89 (2006) 161502.
[12] I.V. Schweigert, Phys. Rev. Lett. 92 (2004) 155001.
[13] J.J. Shi, M.G. Kong, Appl. Phys. Lett. 87 (2005) 101502.